NASA/TM-20240000936

A Phenomenological Durability Model for Environmental Barrier Coating Systems Subjected to Steam Oxidation

Subodh K. Mital
The University of Toledo, Toledo, Ohio

Steven M. Arnold
Glenn Research Center, Cleveland, Ohio

March 2024

NASA STI Program Report Series

Since its founding, NASA has been dedicated to the advancement of aeronautics and space science. The NASA scientific and technical information (STI) program plays a key part in helping NASA maintain this important role.

The NASA STI program operates under the auspices of the Agency Chief Information Officer. It collects, organizes, provides for archiving, and disseminates NASA's STI. The NASA STI program provides access to the NTRS Registered and its public interface, the NASA Technical Reports Server, thus providing one of the largest collections of aeronautical and space science STI in the world. Results are published in both non-NASA channels and by NASA in the NASA STI Report Series, which includes the following report types:

- TECHNICAL PUBLICATION.
  Reports of completed research or a major significant phase of research that present the results of NASA Programs and include extensive data or theoretical analysis. Includes compilations of significant scientific and technical data and information deemed to be of continuing reference value. NASA counterpart of peer-reviewed formal professional papers but has less stringent limitations on manuscript length and extent of graphic presentations.

- TECHNICAL MEMORANDUM.
  Scientific and technical findings that are preliminary or of specialized interest, e.g., quick release reports, working papers, and bibliographies that contain minimal annotation. Does not contain extensive analysis.

- CONTRACTOR REPORT.
  Scientific and technical findings by NASA-sponsored contractors and grantees.

- CONTRACTOR REPORT.
  Scientific and technical findings by NASA-sponsored contractors and grantees.

- CONFERENCE PUBLICATION.
  Collected papers from scientific and technical conferences, symposia, seminars, or other meetings sponsored or co-sponsored by NASA.

- SPECIAL PUBLICATION.
  Scientific, technical, or historical information from NASA programs, projects, and missions, often concerned with subjects having substantial public interest.

- TECHNICAL TRANSLATION.
  English-language translations of foreign scientific and technical material pertinent to NASA's mission.

Specialized services also include organizing and publishing research results, distributing specialized research announcements and feeds, providing information desk and personal search support, and enabling data exchange services.

For more information about the NASA STI program, see the following:

- Access the NASA STI program home page at http://www.sti.nasa.gov

NASA/TM-20240000936

A Phenomenological Durability Model for Environmental Barrier Coating Systems Subjected to Steam Oxidation

Subodh K. Mital
The University of Toledo, Toledo, Ohio

Steven M. Arnold
Glenn Research Center, Cleveland, Ohio

National Aeronautics and
Space Administration

Glenn Research Center
Cleveland, Ohio 44135

March 2024

Acknowledgments

The authors like to thank Bryan Harder, Environmental Effects and Coatings Branch and Josh Stuckner, Multiscale and Multiphysics Modeling Branch at NASA Glenn Research Center for many helpful technical discussions. This work was sponsored by Transformational Tools and Technologies (TTT) project under Transformative Aeronautics Concepts Program (TACP).

This report contains preliminary findings, subject to revision as analysis proceeds.

Level of Review: This material has been technically reviewed by technical management.

This report is available in electronic form at https://www.sti.nasa.gov/ and https://ntrs.nasa.gov/

NASA STI Program/Mail Stop 050
NASA Langley Research Center
Hampton, VA 23681-2199

A Phenomenological Durability Model for Environmental Barrier Coating Systems Subjected to Steam Oxidation

Subodh K. Mital
The University of Toledo
Toledo, Ohio 43606

Steven M. Arnold
National Aeronautics and Space Administration
Glenn Research Center
Cleveland, Ohio 44135

Abstract

Environmental barrier coatings (EBC) are used to protect the silicon carbide fiber reinforced silicon carbide matrix (SiC/SiC) ceramic matrix composites (CMC) from rapid surface recession due to volatization by water vapor in a steam oxidation environment. A phenomenological modeling approach is outlined to estimate the durability of a given EBC system when exposed to steam oxidation. The report provides a step-by-step procedure to estimate the life of a given EBC system subjected to thermal loads only. Once calibrated, the methodology can predict the critical thickness of an oxide layer that will cause failure initiation/spallation as well as the remaining strength or stress that the EBC system can take for a given oxide layer thickness.

Introduction

Ceramic matrix composites (CMC) are being developed as the next generation of materials for use in the hot sections of a gas turbine engine. They offer significant benefits compared to the superalloys currently in use, i.e., lower density and higher temperature capability leading to higher engine efficiency in terms of lower fuel burn and lower emissions (Refs. 1 and 2). The use temperature of the CMCs can be 150 to 200 °C higher than that for metallic superalloys like Inconel, but at one-third the density. This unique combination of properties has helped newer jet engines like the LEAP engine run hotter with less cooling, improving efficiency so that 15 to 20 percent less fuel is burned, with lower emissions and maintenance. It is reported that the GE9X engine, with five CMC parts, will reportedly be the most fuel-efficient engine ever built for a commercial aircraft when the Boeing 777X enters service in 2025 (Ref. 3).

However, the use of these advanced materials also presents some unique challenges. SiC oxidizes to silica (SiO_2) in the gas turbine environment i.e., in the presence of oxygen and/or water vapor. Silica reacts with water vapor and convers to $Si(OH)_4$ which is a gaseous species. This process leads to rapid recession and loss of material. The environmental barrier coatings (EBC) that are used to protect the CMC from oxidation/recession and are generally considered an enabling technology for the successful implementation of CMCs in the next generation of gas turbine engines. Therefore, EBC durability is very critical because EBC failure leads to a rapid reduction of CMC component life. The EBC also provides thermal protection, but its main objective is to provide environmental protection by impeding access of oxidizing species to the underlying SiC component while maintaining adherence over long durations, typically tens of thousands of hours of operation. Because the TGO/EBC assemblage must act as a barrier to the permeation of O_2 and H_2O, the layers must be dense. To minimize thermal stresses that could

induce cracking requires minimization of the mismatch in coefficient of thermal expansion (CTE) with the substrate. This CTE matching restriction limits the choices for EBCs largely to silicate systems, all of which are susceptible to SiO_2 volatilization to some extent depending on their SiO_2 activity.

EBC systems have many failure modes as shown in Figure 1 (Refs. 4 and 5). Key contributors to EBC failure include oxygen-induced oxidation, water-vapor-induced oxidation, water-vapor-induced recession, degradation by calcium-magnesium-aluminum-silicate (CMAS) deposits, thermomechanical strains, particle erosion, and foreign object damage (FOD). Synergies between extrinsic failure modes determine EBC lifetime and design requirements (Ref. 4). Finally, all these mechanisms coalesce into thermomechanical durability. However, in this work we are only focusing on steam oxidation that leads to growth of a silica layer, sometimes referred to as thermally grown oxide (TGO). TGO grows out of a silicon (Si) bond coat (if present) or from a SiC substrate. With time, the oxide layer grows in thickness, and it has been observed that under thermal cycling conditions the EBC spalls from CMC substrate once the TGO layer reaches a critical thickness usually between 20 to 30 μm (Ref. 6).

The stresses or the driving forces in the EBC systems are generated primarily due to coefficient of thermal expansion (CTE) mismatch between various EBC layers and substrate. EBC intrinsic requirements are CTE match, phase stability and no EBC/CMC interaction. In other words, minimizing the CTE mismatch between various layers along with the thermochemical stability is a key design consideration for EBC systems. The objective of the present work is to describe a pragmatic engineering (phenomenological model) approach to estimate the in-situ residual stress state (which is a function of constituent properties and geometry) and thus the critical TGO layer thickness (i.e., lifetime) that induces spallation and failure of the EBC system when subjected to thermal loads only. Results, based on the analysis of a particular EBC system, indicate that a single allowable interfacial strength value can be used to predict damage failure/spallation of the EBC system. If the EBC system is also subjected to mechanical loads, then failure will occur prior to reaching the critical (thermal cycling alone) oxide layer thickness depending upon the magnitude of the applied mechanical load.

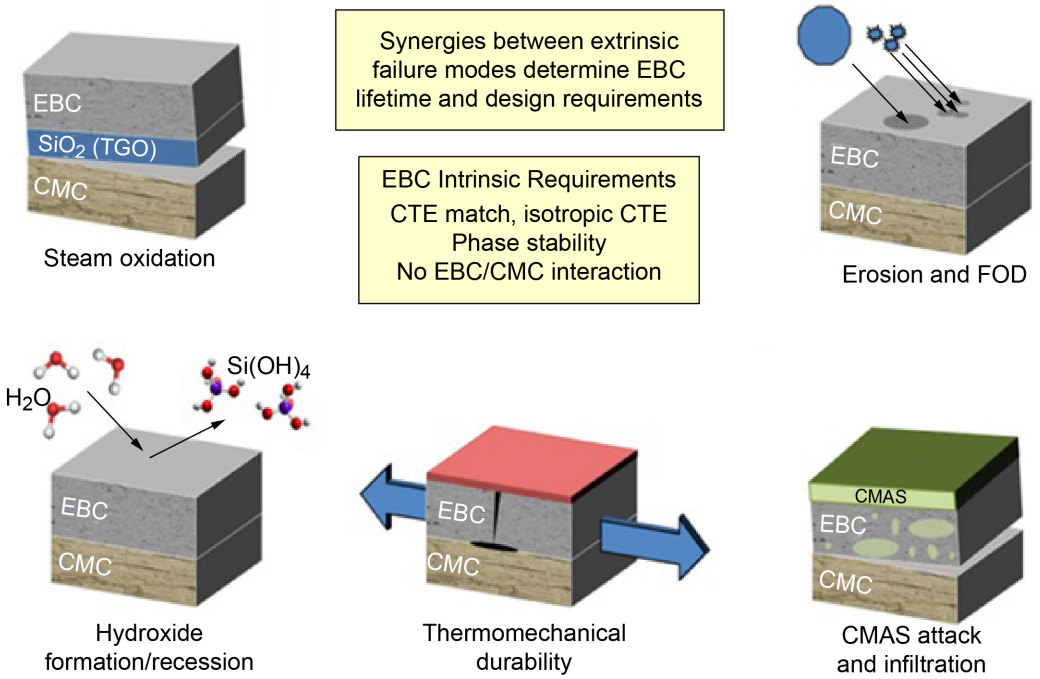

Figure 1.—Failure modes of EBC systems.

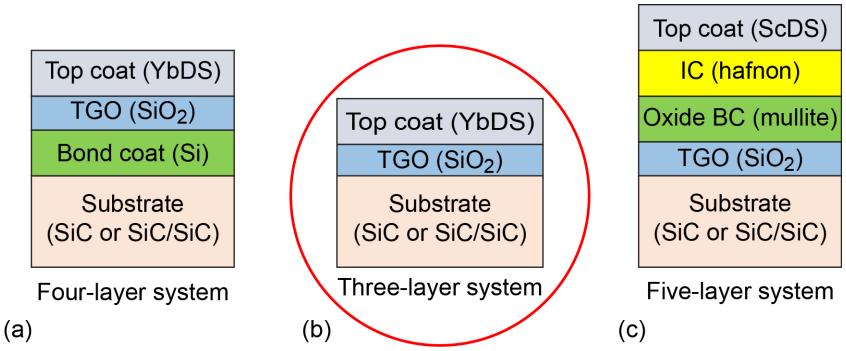

Figure 2.—EBC systems nomenclature (a) Gen 2 (2,400 °F) system. (b) Early (2,700 °F) system. (c) Gen-3 NASA EBC base architecture (3,000 °F). (YDS – ytterbium disilicate; Si – silicon; ScDS – Scandium disilicate; IC – intermediate coat; BC – bond coat; SiC – monolithic silicon carbide (Hexoloy); SiC/SiC – CMC composite with silicon carbide fiber and silicon carbide matrix.)

Nomenclature of EBC Systems

EBC development has been underway for many years. First generation of EBCs were developed in the 1990s under NASA's High Speed Civil Transport—Enabling Propulsion Materials (HSCT-EPM) program. These EBC systems consisted of mullite and BSAS materials. Second generation EBCs were developed under NASA's Ultra Efficient Engine Technology (UEET) program in early 2000s (Ref. 4). Most of the current EBCs are variations of the second generation EBC systems. Figure 2 shows the currently accepted EBC systems nomenclature. The Gen-2 system has a silicon bond coat and an ytterbium di-silicate (YbDS) topcoat. It's use temperature is limited to 1315 °C (2400 °F) due to the presence of the silicon bond coat which has a melting temperature of 1410 °C. Within NASA GRC it is referred to as a four-layer (substrate/bond coat/TGO/topcoat) system. There have been some modifications of these systems by modifying the chemistry of the topcoat wherein slower TGO growth has been demonstrated and thus longer life as compared to the original system (Ref. 7). The EBC system referred to as the early 2700 °F system removed the silicon bond coat as it was limiting the use temperature of the EBC system. As the name suggest, this system has a use temperature up to 1482 °C (2700 °F) when applied to a 1315 °C (2400 °F) capable CMC substrate. This system has also been referred to as a three-layer system (substrate/TGO/topcoat). Some of the newest EBC systems under development are so-called Gen-3 EBC systems that have a potential use temperature up to 3000 °F (1650 °C) if applied on a 2700 °F (1482 °C) capable CMC substrate. These Gen-3 systems, in the base architecture, typically have five layers (substrate/TGO/bond coat/intermediate coat/topcoat). The bond coat in these systems is an oxide-based material (mullite) and intermediate coat is Hafnon ($HfSiO_4$; Hafnium silicate), while the topcoat is Scandium disilicate (ScDS). In another variation of this system, the topcoat is Hafnia (HfO_2) and in yet another variation, the topcoat consists of a hafnia layer over a scandia layer.

Observations From Analyses of Early EBC Systems

Analyses were performed previously on 2400 °F Gen-2 EBC systems (four-layer systems) as well as early 2700 °F systems (three-layer systems) subjected to an isothermal cooldown from a high temperature to room-temperature (Refs. 8 and 9). The TGO grows when the bond coat or the substrate is oxidized at very high temperatures in the presence of oxygen and/or water vapor. Further, it was observed that when these systems are subjected to realistic thermal cycling, the oxide (TGO) layer is in compression in the in-plane direction during the heat up portion of the cycle. Chemical reactions at high temperature cause the

oxide layer thickness to increase during the time the EBC is at high temperature and there is a volumetric change associated with this conversion of bond coat/substrate to TGO. However, the associated thermal chemical induced stresses are quickly relaxed out as these materials, particularly the TGO material, exhibit very high creep rates (Refs. 10 and 11) at temperature as well.

However, during cooldown, tensile stresses develop in the oxide layer, which in conjunction with coating interface roughness and prior damage will induce further initiation/propagation of damage within the TGO and interface surfaces. The damage in the form of vertical cracks in the oxide layer is modeled explicitly in these analyses. However, there are other types of damage in the system such as horizontal cracks, porosity etc. which is not modeled explicitly but their effects are accounted for lowering the layer stiffness. The resulting stress-state in the oxide layer from these analyses can be summarized as follows:

1. Out of plane peel (that cause delamination/cracking) and shear stresses (that drive the delamination) are minimal for uniform layers with no damage. Only in-plane tensile stresses are present which cause self-similar vertical cracks to develop as the TGO grows.
2. In-plane stresses (that cause vertical cracks) are high and are primarily driven by CTE mismatch. They are independent of the oxide layer thickness and only increase slightly in the presence of nonuniformity/damage.
3. In real systems, damage, in the form of vertical cracks in the oxide layer, are always present. TGO layers are also highly nonuniform in thickness.
4. Shear stresses are high in the presence of damage (e.g., vertical cracks) and increase only slightly with increase in oxide layer thickness or with increasing nonuniformity.
5. Peel stress is present in the presence of damage and increases rapidly with the introduction of even a slight nonuniformity (or roughness) of TGO. Peel stress also increases with increasing oxide layer thickness.
6. As these systems are cooled from a high temperature to room temperature, the stresses that develop quickly relax out due to the assumed high creep rate of these materials as mentioned before. To perform an actual creep/relaxation analysis, the creep rates of all constituent materials as a function of stress and temperature are required. Similarly, one must know the time temperature profile of the cooling applied to the EBC system. Usually, such information is not readily available. Further, such calculations are extremely computationally expensive as the finite element meshes of these systems are relatively large and the time increments very small. Consequently, one can use a lower “stress-free” temperature (much lower than the temperature at which the coating is applied) and perform a simple elastic time-independent analysis to obtain reasonably accurate residual stress states. The value of this “stress-free” temperature is chosen in a way that will result in the stress state at room-temperature being similar to that if a full-scale creep/relaxation analysis would have been performed (Ref. 12).

Figure 3 shows maximum in-plane, peel, and shear stresses for an early 2700 °F system under isothermal cooldown from a stress-free temperature of 500 °C to room temperature based on 2-D plane stress finite element analyses. The stresses are plotted as a function of nonuniformity as defined by the parameter R, which is the ratio of minimum oxide layer thickness to the nominal thickness. Thus, R = 1 implied uniform oxide layer thickness and R = 0 implies very severe nonuniformity with islands of oxide layer. The location of these maximum not always being the same. In these analyses, a monolithic, isotropic, silicon carbide material, Hexoloy®[1], has been used as the substrate material. The resulting

[1]Hexoloy® SA alpha silicon carbide, Carborandum/St. Gobain, Niagara Falls, NY

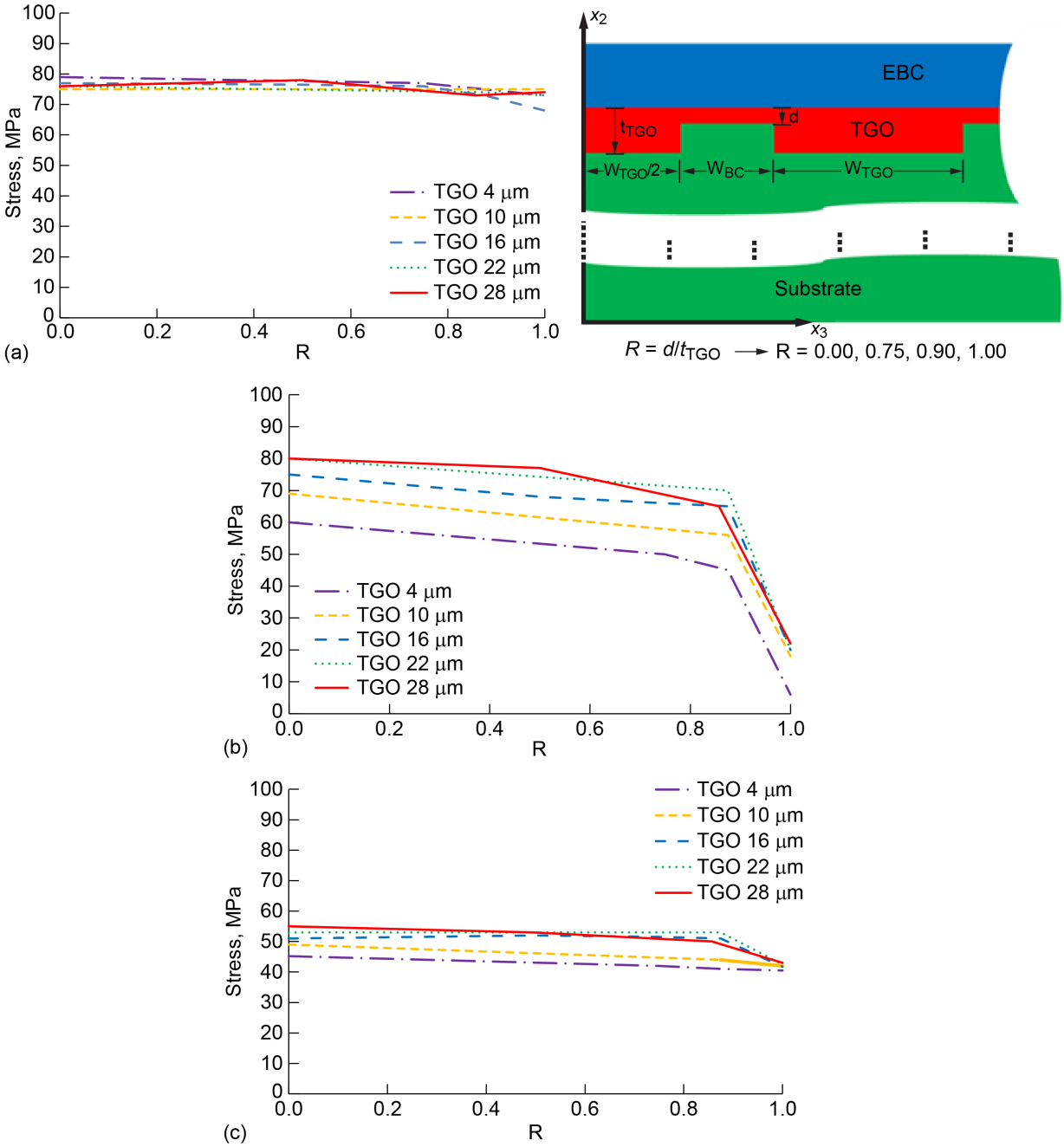

Figure 3.—Driving forces (stress) as a function of TGO roughness and thickness for early 2700 °F system; (a) in-plane (severity of nonuniformity considered by adjusted R factor), (b) peel stress (maximum peel stress in TGO layer cracks at 10 μm spacing, ΔT = 500 °C), (c) shear stresses (maximum shear stress in TGO layer cracks at 10 μm spacing, ΔT = 500 °C) (Refs. 8 and 9).

driving forces, specifically peel and shear stresses, depend upon not only on material properties and damage (vertical crack spacing), but most importantly on EBC architecture, i.e., layer thickness and roughness (nonuniformity) of the oxide layer. In-plane stresses (the cause of vertical cracking) in the oxide layer are relatively constant and independent of TGO thickness and nonuniformity (roughness). Given these results, the tensile strength of the oxide (TGO) material appears to be approximately 80 MPa, given this stress-free temperature.

Figure 4 and Figure 5 show the stress contours (J_2, σ_{11}, σ_{22}, σ_{12}, I_1) for two cases—one with an oxide layer thickness of 16 µm and R = 0.5 (see Figure 4) and the other one with an oxide layer thickness of 22 µm and R = 0 (see Figure 5). Both cases have vertical cracks, 10 µm apart, in the oxide layer. Note

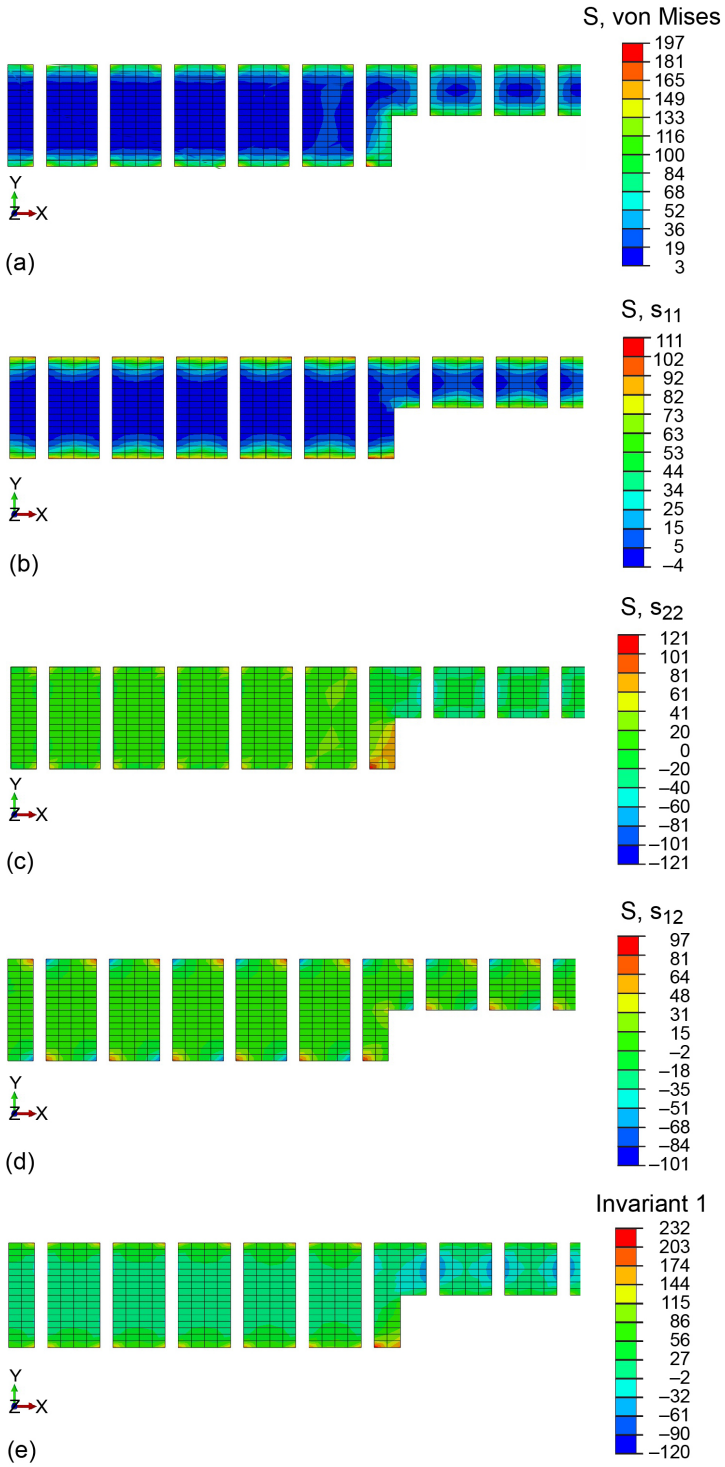

Figure 4.—Stress contours (MPa) in the oxide layer in a EBC system with 16 µm thick oxide layer and R = 0.5, left edge of the image is centerline. (a) J_2, (b) σ_{11}, (c) σ_{22}, (d) σ_{12}, and (e) I_1.

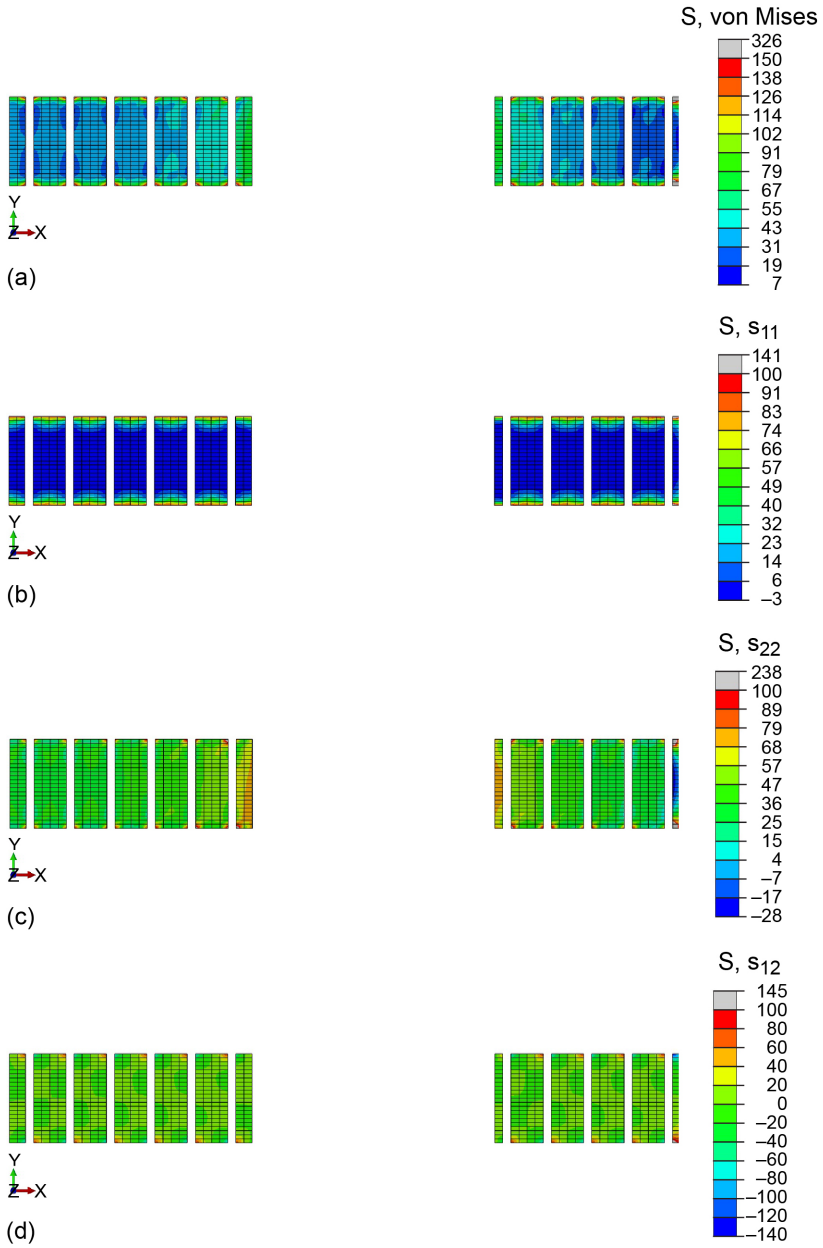

Figure 5.—Stress contours (MPa) in the oxide layer in a EBC system with 22 μm thick oxide layer and R = 0.0, left edge of the image is centerline. (a) J_2, (b) σ_{11}, (c) σ_{22}, and (d) σ_{12}.

that the material layers above (topcoat) and below (substrate) the TGO are not shown in the figures but were present in the calculations. Results show that stresses are generally maximum at the crack tips and at the corners (idealized by zeroing out the stiffness of a column of elements every 10 μm) and usually at the TGO/substrate interface located along the bottom edge of the contour plots.

Phenomenological Modeling Approach

Here a phenomenological modeling approach is outlined to provide an estimate of the in-situ residual stress state (which is a function of constituent properties and geometry) and thus critical thickness of the oxide layer that will cause spallation of a given EBC system when subjected to thermal loads only. This

approach, which consists of seven steps is outlined here, and will be explained in the next section by using the example of an early 2700 °F system.

1. Define the system to be modeled—First the architecture (constituent materials and geometry) of the system that is being modeled must be identified and defined. For example, it could be Gen-2 EBC system or a modified Gen-2 EBC system etc.
2. Obtain a consistent set of material properties—One must obtain a set of material properties for each material in the system e.g., Young's modulus, Poisson's ratio, and coefficient of thermal expansion (CTE), each as a function of temperature. If possible and available, time-dependent properties or creep rates for each material as a function of temperature and stress level are also useful, although they are not always easily available. If unavailable, one can perform an elastic analysis using the concept of stress-free temperature. This assumes that above the stress-free temperature, stresses do not build up because they relax out as fast as they are generated (clearly this is dependent upon the rate of cooling).
3. Characterize the roughness and damage in the oxide layer—since the local stresses depend upon the damage (vertical cracks, porosity, etc.) and the roughness of the TGO layer, it is critical to characterize these for a given EBC system and for a given exposure time. Exposure time is also crucial as the TGO layer thickness is a function of exposure time, i.e., time at temperature. To characterize the damage (generally in the form of vertical cracks in the oxide layer) as well as the roughness or the nonuniformity of the oxide layer, one needs a set of micrographs from a test sample. Information such as average oxide layer thickness and roughness and the related statistics need to be extracted from those micrographs. One way to achieve that is to use a convolutional neural network and extract relevant features from the micrographs as shown in Figure 6. A set of python instructions are provided in Reference 13 to perform such analyses and results have been documented in Reference 14. Usually, hundreds of images are required across a test specimen to obtain a statistical distribution of those required features.
4. Knowing the nonuniformity and average crack spacing in the TGO layer, one can compute the peel and shear stresses from "design curves" such as those shown in Figure 3 which are established by running numerous computations utilizing this microstructural information. These curves provide "residual stresses" as a function of microstructure and cooldown from a stress-free temperature to room-temperature.
5. In-situ interface failure allowables are inferred from pull tests or flatwise tension tests on a given EBC system- given the applied load/stress at failure for the given oxide layer thickness. Since this is the applied global load/stress, it must be converted to in-situ stress at failure or in-situ strength by multiplying the applied global stress by a magnification factor (MF). The value of this magnification factor depends upon the TGO microstructure for the EBC system under consideration, i.e., layer thickness, level of nonuniformity, etc.
6. Repeat the above step for a different exposure time and thus a different TGO thickness and compute the in-situ interfacial strength. Often, a single value of interfacial in-situ strength can be used to estimate the critical oxide layer thickness. Note this strength has associated with it a given volume of material in which both initiation and propagation of damage are assumed to have occurred within - thus the phenomenological nature of the method.
7. This value will help to determine critical TGO thickness where cracks join, driven by local shear stresses, to ultimately cause spallation of the coating.

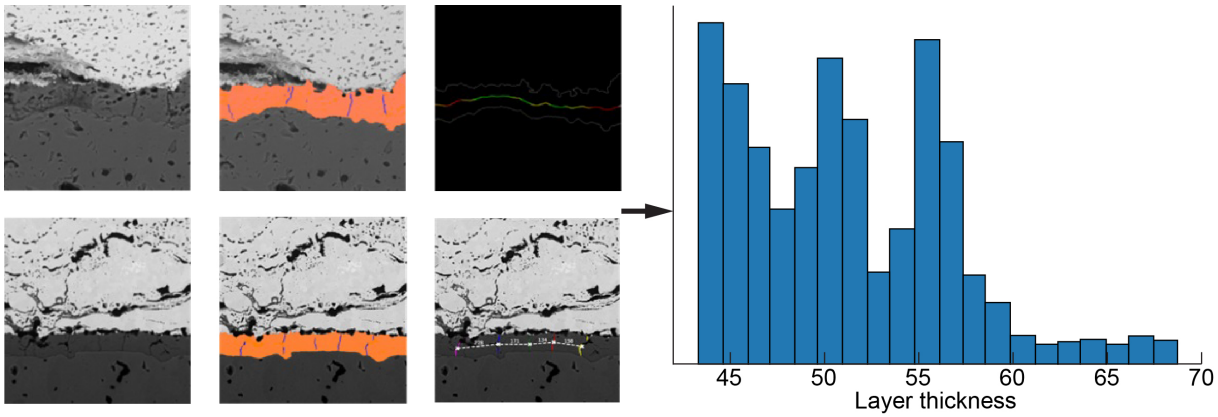

Figure 6.—Extraction of oxide layer features from micrographs of specimens (Ref. 14).

Du et al. (Ref. 15) have also performed a comprehensive study and modeled the effects of the TGO and interfacial roughness on the stress distribution in EBCs. However, they have not accounted for the damage in the oxide layer in the form of vertical cracks that are always present as well as stress relaxation that occurs due to creep in EBC layers. The damage in the oxide layer and creep/relaxation totally changes the nature of the stress distribution in EBCs and thus their results cannot be compared with the results from the present study.

Furthermore, it is imperative that modelers strive to understand exactly how a given experiment was conducted to ensure proper interpretation of the results and *idealization consistency*. Many interdependent factors are comprised within the concept of idealization consistency and can be classified into three main categories: theoretical, mechanistic, and numerical consistencies. *Theoretical consistency* requires preserving the mathematical aspects (e.g., theory, model dimensionality, functional form, etc.) used throughout characterization to prediction. *Mechanistic consistency* would be associated with assumed measures and definitions of damage and modes of failure and their interactions which should be accounted for not only in the final prediction but also during characterization. Length scale (e.g., material volume element) and mesh accuracy are both examples that would fall within the *numerical consistency* category and thus the preservation of these accuracies from characterization to prediction is important. It is important to remember that these categories are typically not mutually exclusive and thus the influence of one on another is often difficult to explicitly determine. This is particularly true in the case of multiscale analysis wherein all factors can interact aggressively as one traverses various length scales (Ref. 16).

In the next section, the above steps will be explained with the help of an example.

Example of Early 2700 °F EBC System

These steps will be demonstrated here using an early 2700 °F system with a SiC (Hexoloy®) substrate. A stress-free temperature of 500 °C has been assumed (based off the temperature dependent creep rates of the constituents) and the specimens are cooled in an isothermal manner from this stress-free temperature to room temperature. The nontemperature dependent thermomechanical properties used for various materials in this EBC system are shown in Table I. Temperature dependent properties within this range make only slight changes in the resulting stress calculations, i.e., <5 percent.

EBC coated samples were exposed to 1426 °C in 90 percent H_2O in a continuous exposure with no cycling. Specimens were imaged from one end to the other (~140 images for a 1-in. diameter specimen). For each image, multiple measurements were taken of oxide layer thickness, roughness etc. and the following statistics were obtained for two exposure times 49 and 100 h. These statistics are shown in Table II.

TABLE I.—MATERIAL PROPERTIES (RT–500 °C)

Material	Young's modulus GPa	Poisson's ratio	Coefficient of thermal expansion 10^{-6}/°C
Topcoat	200	0.27	4.5
TGO	35	0.17	10
Substrate	400	0.17	5.25

TABLE II.—OXIDE LAYER MEASUREMENTS AND STATISTICS

Property	49 h exposure	100 h exposure
Average thickness, μm	4.3	9.8
Standard deviation, μm	1.42	2.96
Coefficient of variation	0.3	0.3
Minimum thickness, μm	1.64	2.6
Maximum thickness, μm	13.8	23.5
Average roughness-top, μm	2.15	2.23
Average roughness-bottom, μm	1.99	1.94
Total roughness, μm	4.14	4.17

TABLE III.—MAXIMUM INTERFACIAL STRESSES

	R = 0.4		R = 0.27	
TGO average thickness μm	Peel stress MPa	Shear stress MPa	Peel stress MPa	Shear stress MPa
4.3	55	44	--	--
9.8	--	--	67	46

As one can see from Table II, there is tremendous variation in the oxide layer thickness and roughness profile. The roughness in the model is defined as the ratio of minimum oxide layer thickness to the nominal (average) thickness. Based on this definition, the R for 49 h of exposure is computed as 1.64/4.3 = 0.4 as the worst-case scenario, while for the 100 h exposure time, it is 2.6/9.8 = 0.27. Based on these R values and oxide layer thickness, one can "read" the peel and shear stresses from the design curves shown in Figure 3. Those extracted are shown in Table III.

These stresses are compared to the strengths that are obtained by performing a flatwise tension test on these specimens. For this early 2700 °F system, Figure 7 shows the strength of the TGO interface as a function of oxide layer thickness. These tests are done at room-temperature, so the layers in the specimen have residual stresses due to the cooldown from a high temperature to room-temperature.

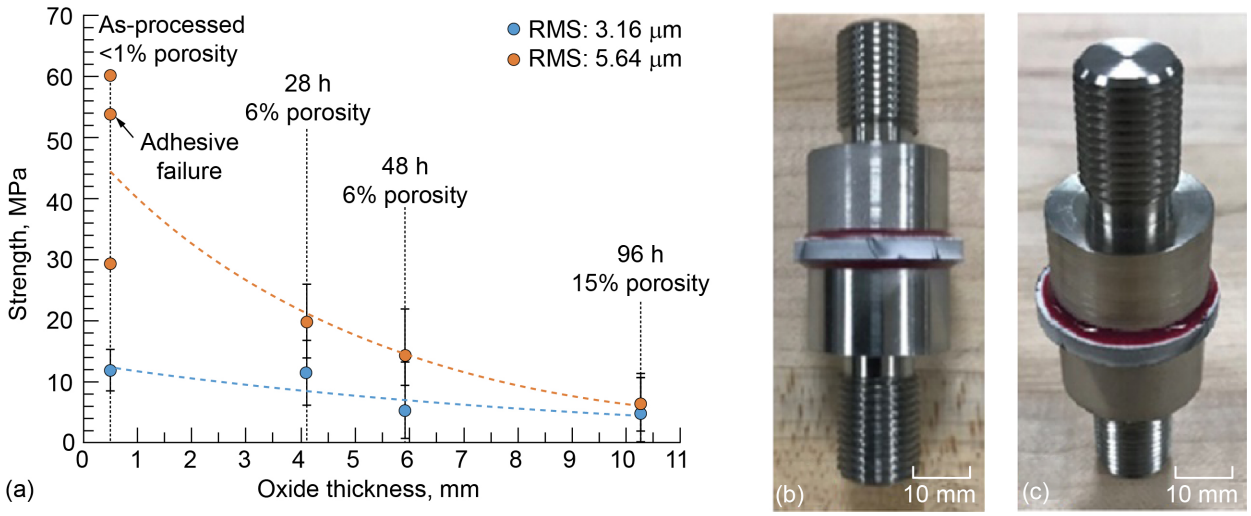

Figure 7.—EBC strength as a function of oxide layer thickness.

Details on how these strength tests are performed are provided in References 17 and 18. The specimen geometry is also shown in the upper right corner of Figure 7. Strength values show a fair amount of scatter. It also appears that the effect of initial roughness is not important after the oxide layer thickness is greater than 10 μm for the average strength value. This scatter in measured strength can possibly be due to large scatter in oxide layer thickness and nonuniformity. However, the strength shown in Figure 7 is merely the magnitude of the applied global stress (applied load at failure/tab cross-sectional area) at which the specimen failed (residual strength). It is not the in-situ stress at failure near the oxide layer interfaces. Analyses have shown that in-situ peel and shear stresses are anywhere from 3 to 5 times (magnification factor) of the applied global stresses depending upon the oxide layer thickness and the level of nonuniformity (roughness) with a given damage in the form of vertical cracks in the oxide layer at an average distance of 10 μm apart. Note as stated before this strength inherently also assumes a given volume of material over which failure has initiated and propagated (or in other words full separation of specimen occurred). The area is 0.75 in^2.

It appears, from Figure 7, that for a 4 μm thick oxide layer, the average value of measured strength is approximately 15 MPa. Residual peel stresses are 55 MPa as shown in Table III. Therefore, the actual interfacial strength is approximately 15 × 3.5 (magnification factor given R = 0.4) + 55 = 107.5 MPa with a lower bound value of 97 MPa and upper bound value of 132 MPa given the scatter in measured strength. If one performs a similar calculation for the specimen with average oxide layer thickness of 10 μm, the average measured strength is approximately 10 MPa. Therefore, the actual interfacial strength is approximately 10 × 4 (magnification factor for a R value of 0.27+67 (residual peel stress due to cooldown) = 107 MPa with a lower bound value of 75 MPa and an upper bound value of 115 MPa. Based on the average values, these results show that a single allowable in-situ interfacial strength value of approximately 107 MPa (with a range of 75 to 132 MPa) can be used to predict critical TGO thickness (one that is due to thermal loading only) that will cause failure initiation/spallation of approximately 0.75 in^2 of EBC from the substrate. Alternatively, one can also apply an in-plane global load in combination with thermal cooldown to obtain critical thicknesses associated with a given applied mechanical loading.

Figure 8 shows a typical TGO growth curve in steam environment (Refs. 19 and 20). This curve is shown for schematic purposes only and is not necessarily for the EBC system under consideration here. It should be noted that such a curve is specific to an EBC system and environment (e.g., temperature,

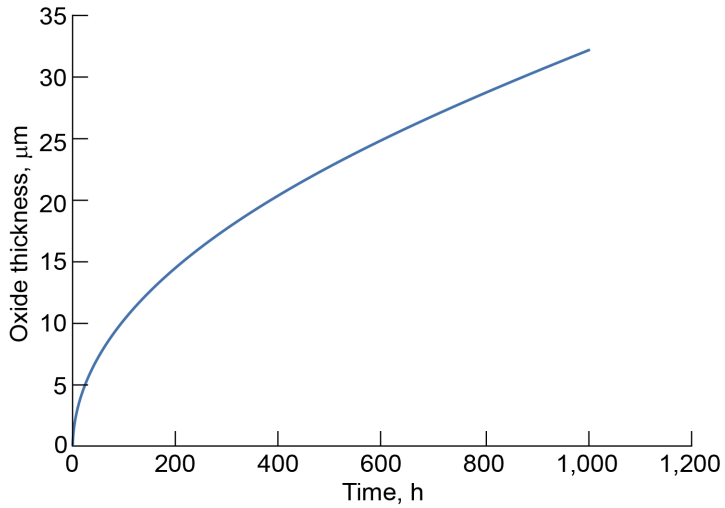

Figure 8.—Typical TGO growth curve in steam environment (Ref. 20).

moisture, architecture etc.). Once the value of the critical TGO thickness that will cause initial failure/spallation over a given area is known, it can be converted to the time in hours using a TGO growth curve like the one shown above in Figure 8.

The following example demonstrates how the failure of EBC/TGO can be predicted using an average strength value of 107 MPa computed above and a stress-free temperature. It must be emphasized again that the stresses and strength values being used here are very specific to an EBC system as well as environment (in particular, temperature and moisture). Let's say the average thickness of oxide layer is 16 µm after a certain time of thermal exposure. Let's say that nonuniformity or roughness as indicated by the parameter R is equal to 0.15. The peel stress for these values is 75 MPa as shown by design curves in Figure 5. That means the remaining interfacial strength is equal to 107 – 75 = 32 MPa. Assuming a magnification factor of 4 between in-situ interfacial stress versus applied global stress, the remaining external load/pressure is 32/4 = 8 MPa. Consequently, if one were to conduct a flatwise tension test of this EBC system like the one shown in Figure 7, it would fail at an applied global stress of 8 MPa on average. Thus, once the in-situ stress in the oxide layer reaches the strength value (80 MPa in this system), the oxide layer itself can fail even though the interface may be intact. On the other hand, if the interfacial peel stress reaches the interfacial strength, delamination/failure initiates and the high shear stress can cause that failure to propagate, leading to spallation of the EBC from substrate.

Summary

In this paper, a phenomenological, pragmatic modeling approach to estimate the failure strength of EBC systems, subjected to thermal loads only, ΔT, given the thickness, roughness, and damage state of the oxide layer, architecture of the system, and constituent properties was outlined. It was shown that for a given system, one needs to generate the driving forces (stress) curves as a function of oxide layer thickness and nonuniformity for both thermal only and thermomechanical loadings. It was found that damage (vertical cracking) in the oxide layer always occurs during cooldown from a high temperature to room temperature. In lieu of performing a full creep/relaxation analysis, one can perform a linear elastic analysis assuming a lower stress-free temperature. Out of plane strength curves of the EBC as a function of oxide layer thickness and roughness are also needed. Data from two or more exposure times are needed to calibrate a value of interfacial strength that can be used to obtain an estimate of critical thickness of oxide layer that will initial failure and cause spallation. Given a TGO growth curve for a given system,

one can convert a critical oxide layer thickness to get an estimate of the lifetime of the EBC system in hours. Additionally, these types of materials might exhibit a volume or area effect as many ceramics do. Consequently, the interfacial strength numbers shown here pertain to a 1-in. diameter disc specimen loaded with a 0.85 in. diameter pull tab. For specimens with a bigger area/volume, the strength values may be different. Lastly, the approach also estimates the remaining strength of the EBC systems at any given point. Consequently, if the coating is also subjected to the mechanical stresses, then the EBC system will fail whenever the applied load exceeds the remaining strength.

References

1. J. Steibel, Ceramic matrix composites taking flight at GE Aviation, Am. Ceram. Soc. Bulletin, 98(3), 2019, pp. 30–33.
2. F.W. Zok, Ceramic-matrix composites enable revolutionary gains in turbine engine efficiency, Am. Ceram. Soc. Bulletin, 95(5), 2016.
3. https://www.compositesworld.com/articles/a-new-era-for-ceramic-matrix-composites
4. K.N. Lee, Environmental barrier coatings for CMCs in: N.P. Bansal, J. Lamon (Eds.) Ceramic Matrix Composites, Wiley, New York, 2015, pp. 433–451.
5. Xiao S., Li J., Huang P., Zhang A., Tian Y., Zhang X., et al. Evaluation of environmental barrier coatings: A review. Int J Appl Ceram Technol. 2023; 1–22. https://doi.org/10.1111/ijac.14370
6. M. Presby et al., The development and use of a natural gas/oxygen burner rig for environmental barrier coating and ceramic matrix composite technology maturation, Proc. ASME Turbo Expo 2023, Paper No. GT2023-101562, June 26–30, 2023, Boston, MA.
7. K.N. Lee, $Yb_2Si_2O_7$ Environmental barrier coatings with reduced bond coat oxidation rates via chemical modifications for long life. J. Am. Ceram. Soc., 102(3), 2018, pp. 1507–1521.
8. T.M. Ricks et al., Coupled thermos-mechanical modeling of the influence of the thermally grown oxide in an environmental barrier coating system, Proc. 33rd Am. Soc. Of Composites Annual Technical Conf., Sep. 24–16, 2018, Seattle, WA.
9. S.K. Mital et al., Modeling the influence of thermally grown oxide (TGO) layers on the driving forces in environmental barrier coating systems, NASA/TM-201210014094, April 2021.
10. Richards et al., Mechanical Properties of Air Plasma Sprayed Environmental Barrier Coating (EBC) Systems: Preliminary Assessments," Developments in Strategic Ceramic Materials – A Collection of Papers presented at 39th International Conference of Advanced Ceramics and Composites, Daytona Beach, FL, American Ceramic Society, Dec. 2015.
11. A.A. Wereszczak, et al., Dimensional changes and creep of silica core ceramics used in investment casting of superalloys, J. of Materials Science, vol. 37, 2002, pp. 4235–4245.
12. N.N. Nemeth et al., Stochastic simulation of mudcrack damage formation in an environmental barrier coating, NASA/TP-2020-220185, February 2020.
13. https://github.com/nasa/pretrained-microscopy-models
14. Stuckner, J.; Harder, B.; Smith, T.M. Microstructure segmentation with deep learning encoders pre-trained on a large micros-515 copy dataset. J. Comput. Mater. 2022, 8, pp. 1–12.
15. Jinkang Du et al. Effect of the thermally grown oxide and interfacial roughness on stress distribution in environmental barrier coatings, J. of European Ceramic Society, vol. 43, issue 15, December 2023, pp. 7118–7133. https://doi.org/10.1016/j.jeauceramsoc.2023.07.074
16. P. Naghipour, S. Arnold, S., et al. Multiscale Static Analysis of Notched and Unnotched Laminates Using the Generalized Method of Cells, NASA/TM-2016-219084, 2016.

17. J. Salem et al., Design of an environmental barrier coating bond strength test coupon, Proc. ASME Turbo Expo 2023, GT2023, June 26–20, Boston, MA.
18. B.J. Harder, M.J. Presby, et al. Environmental Barrier Coating Oxidation and Adhesion Strength, J. of Engineering for Gas Turbine and Power, vol. 143, March 2021.
19. Deal, B.E.; and Grove A.S.: General Relationship for the Thermal Oxidation of Silicon. J. Appl. Phys., 1965, vol. 36, no. 12, pp. 3770–3778.
20. Private communication, Roy Sullivan, NASA Glenn Research Center, Cleveland, Ohio, Dec. 2023.